Supporting Information

p-Block Dopant Enables Energy-Efficient Hydrogen Production from Biomass

1. Experimental section

1.1 Chemicals

Cobalt nitrate hexahydrate $(Co(NO_3)_2 \cdot 6H_2O)$, bismuth nitrate pentahydrate $(Bi(NO_3)_3 \cdot 5H_2O)$, glucose, 2-methylimidazole (2-mim), potassium hydroxide (KOH)，commercial ruthenium dioxide (RuO_2, 99.9%), nafion (5 wt%) were purchased from Aladdin (Shanghai, China) , and used without any further purification. The solutions in this work were prepared by methanol (99.9%).

1.2 Preparation of catalysts

1.2.1 Preparation of Bi-Co$_3$O$_4$ NFAs

Nickel foam was carefully pretreated before the experiment: Firstly cut nickel foam into rectangular pieces (3×3 cm^2), then put it in the ultrasound chamber and sonicate it in 3 mol L^{-1} diluted hydrochloric acid (HCl), absolute ethanol, acetone and methanol for 5 min in turn to remove the oxide layer and residual organic matter on the surface.

Firstly, the $Co(NO_3)_2 \cdot 6H_2O$ 1.020 g and $Bi(NO_3)_3 \cdot 5H_2O$ 0.243 g were weighed and dissolved in 15 mL methanol, and then evenly stirred to form solution A; the 2-mim 0.616 g was weighed and dissolved in 15 mL methanol, and evenly stirred to form solution B; the BiCo-mim was prepared by vertically inserting the treated nickel foam into the inner lining of the 50mL reaction kettle; the BiCo-mim was prepared by solvothermal reaction at 120 ℃ for 4 h. The precursor was cooled naturally to room temperature, washed three times with methanol and dried in the vacuum oven at 60 ℃ for 6 h; the precursor was placed in a quartz tube furnace and calcined in air at 350 ℃ for 2 h (heating rate was 10 ℃ min^{-1}) to obtain Bi-Co$_3$O$_4$ NFAs.

1.2.2 Preparation of Co$_3$O$_4$ NFAs

The $Co(NO_3)_2 \cdot 6H_2O$ 1.164 g was weighed and dissolved in 15 mL methanol, and then evenly stirred to form solution A; the 2-mim 0.616 g was weighed and dissolved in 15 mL methanol, and evenly stirred to form solution B; the Co-mim was prepared by

vertically inserting the treated nickel foam into the inner lining of the 50 mL reaction kettle; the Co-mim was prepared by hydrothermal reaction at 120 °C for 4 h. The precursor was cooled naturally to room temperature, washed three times with methanol and dried in the vacuum oven at 60 °C for 6 h; the precursor was placed in a quartz tube furnace and calcined in air at 350 °C for 2 h (heating rate was 10 °C min^{-1}) to obtain Co_3O_4 NFAs.

1.2.3 Preparation of RuO_2/NF

Commercial RuO_2 (2.500 mg) was dispersed into a mixture of 100 μL ethanol, 385 μL ultrapure water and 15 μL Nafion (5 wt%) and sonicated for 30 min to form a uniform ink. Then 100 μL of ink drops were added to the nickel foam and dried under an infrared lamp. The commercial sample has a drop area of 1 cm^2 on nickel foam, which is the same as the area tested for the performance of the electrocatalyst.

1.3 Characterization

The apparent morphology and structure of the materials were characterized using field emission scanning electron microscopy (SEM) (Nova NanoSEM 450, PNAlytical, the Netherlands) and transmission electron microscopy (TEM) (Tecnai G2 F30 STwin, Phlips-FEI, the Netherlands). The crystal structure of the material was characterized by X-ray diffractometer (XRD) (model X 'Pert PRO, PNAlytical, the Netherlands) in the range of 5° to 80°. An X-ray photoelectron spectrometer (XPS) (Thermo Scientific K-Alpha, the Shimadzu Kratos) was used to characterize the chemical properties of the material surface (Al (Ka) radiation as a probe). The carbon peak (C 1s: 284.80 eV) was used to calibrate the binding energy. Raman spectroscopy analyzer (LabRAM HR800, Horiba Jobin Yvon, France) was used to test the chemical structure of the materials. The composition of the electrolyte was analyzed by mass spectrometry (SCIEX X500R QTOF MS).

1.4 Electrochemical measurements

Electrochemical tests were performed on CHI 760e electrochemical workstation. The HER, OER and GOR properties of the catalyst were tested with a three-electrode

system. The sample, carbon rod and saturated calomel electrode (SCE) were used as working electrode, counter electrode and reference electrode, respectively. The measured potentials were converted to reversible hydrogen electrode (RHE), $E_{RHE} = E_{SCE} + 0.242 + 0.059 \times pH$. The electrochemical performance and cycle stability of the catalyst in glucose alkaline solution were tested by two electrodes.

Linear sweep voltammetry (LSV) polarization curves were obtained at 1 M KOH or 1 M KOH + 0.15 M glucose at a sweep rate of 5 mV s^{-1} with 95% IR compensation. Tafel slopes were calculated linear regression using the equation $\eta = b \log|j| + a$, η (V) is the overpotential, j (mA·cm^{-2}) is the current density. The EIS was measured at open circuit voltages and at frequencies ranging from 0.1 to 100000 Hz. The electric double layer capacitance (C_{dl}) was calculated from cyclic voltammograms (CV) obtained in the non-Faraday interval (10 to 50 mV s^{-1}) and used to assess the electrochemical active specific surface area (ECSA).
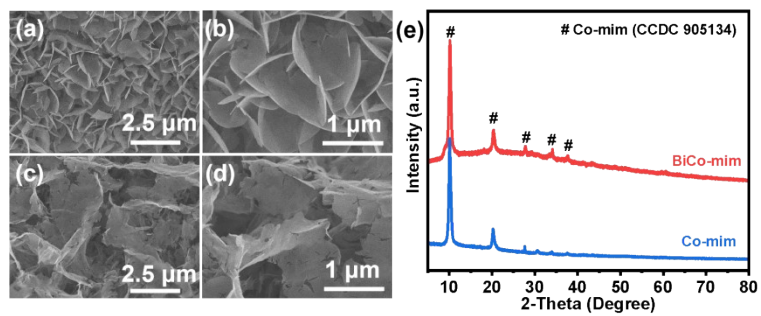
2. Supplementary figures

Fig. S1 SEM images of a, b) Co-mim and c, d) BiCo-mim. e) XRD patterns of Co-mim and BiCo-mim separated from nickel foam.
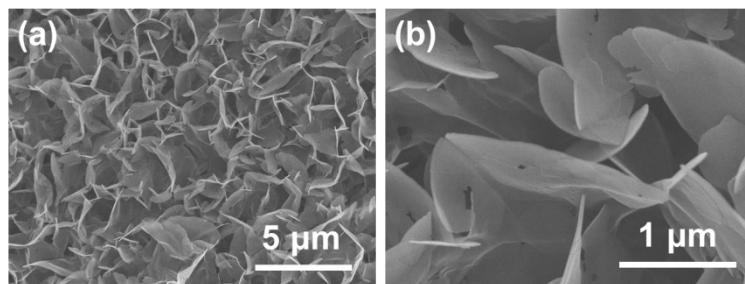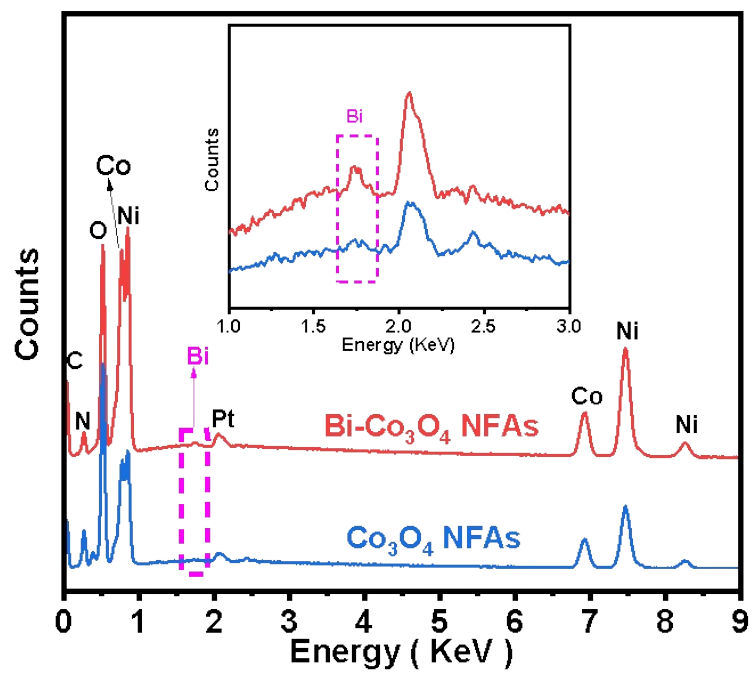
Fig. S2 SEM images of Co_3O_4 NFAs.

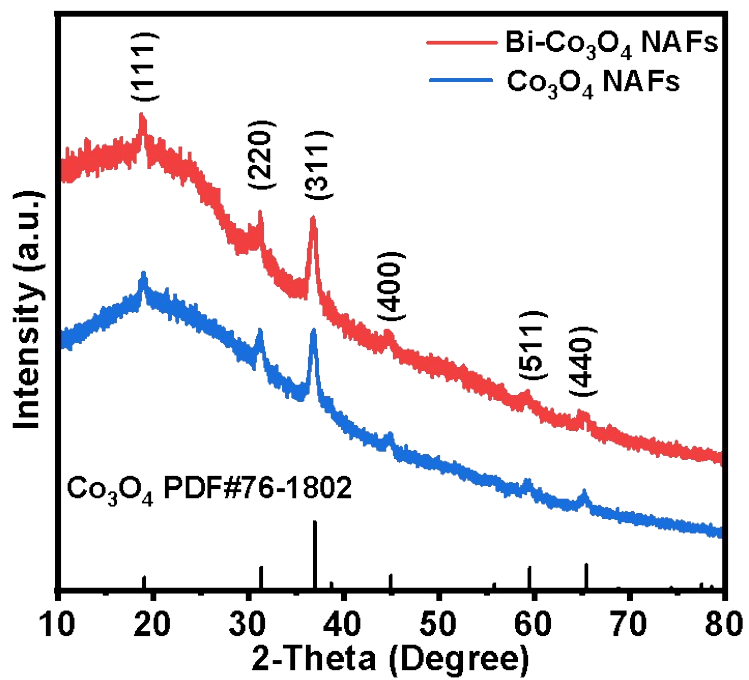**Fig. S3** EDS spectra of Bi-Co_3O_4 NFAs and Co_3O_4 NFAs.

Fig. S4 XRD patterns of Bi-Co_3O_4 NAFs and Co_3O_4 NAFs.
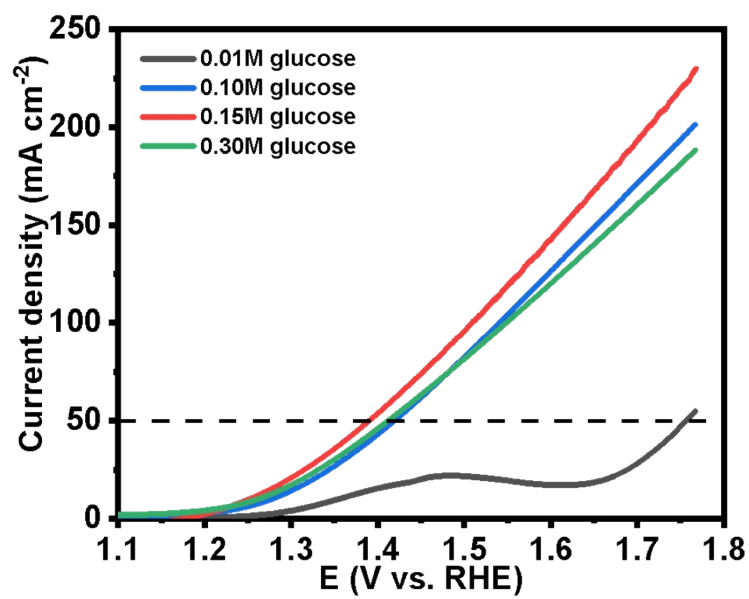
Fig. S5 The GOR polarization curves of Bi-Co$_3$O$_4$ NFAs in different electrolytes.
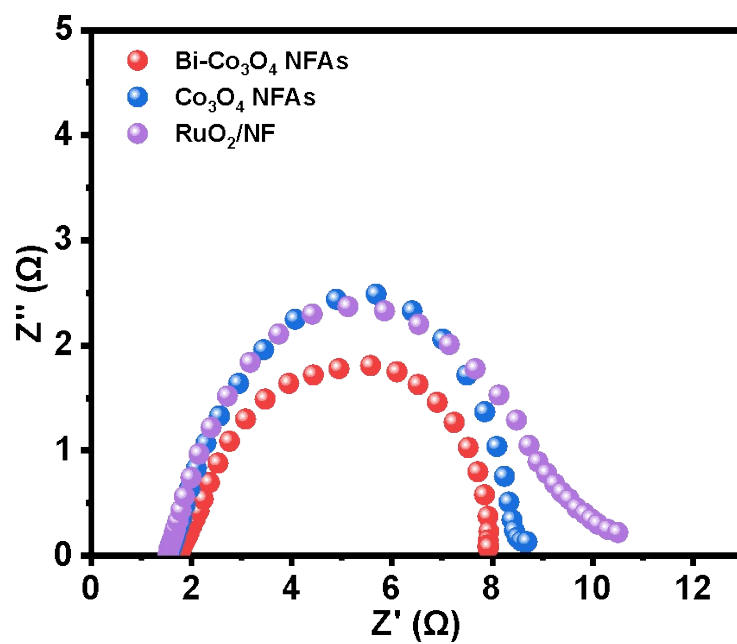
Fig. S6 The Nyquist plots of Bi-Co_3O_4 NFAs, Co_3O_4 NFAs, and RuO_2/NF in 1 M KOH + 0.15 M glucose.
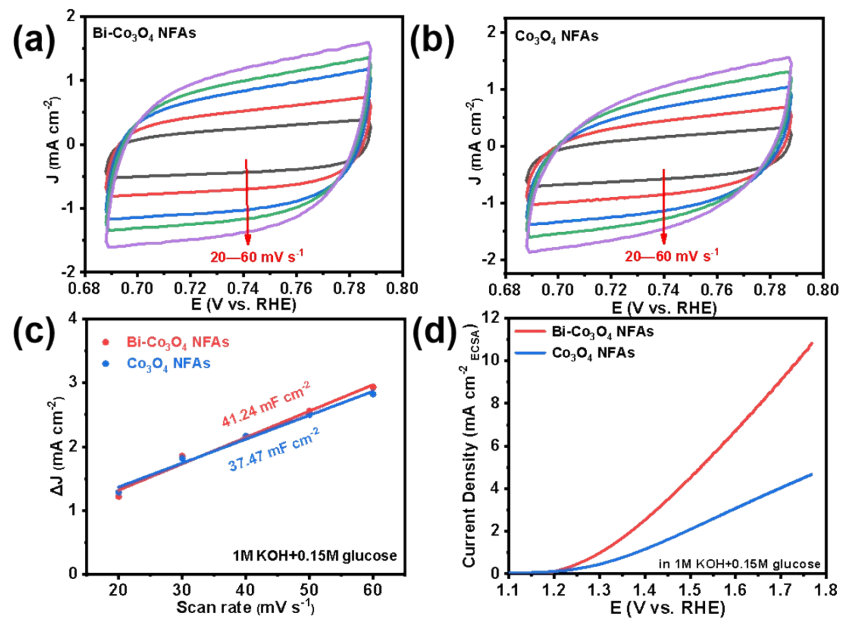
Fig. S7 The C_{dl} curves of a) Bi-Co$_3$O$_4$ NFAs, b) Co$_3$O$_4$ NFAs, and c) the corresponding ECSA curves; d) The ECSA-normalized LSV curves in 1 M KOH + 0.15 M glucose.

Fig. S8 The extraction ion flow chromatography and the corresponding mass spectrometry of the products in the electrolyte after electrolysis: (a) glucose, (b) lactic acid, (c) arabinose, and (d) gluconic acid.

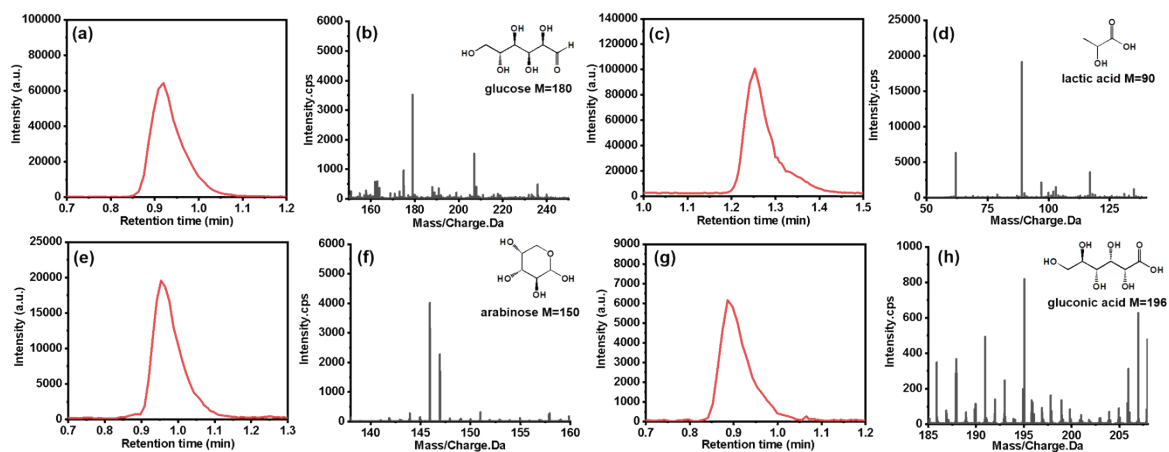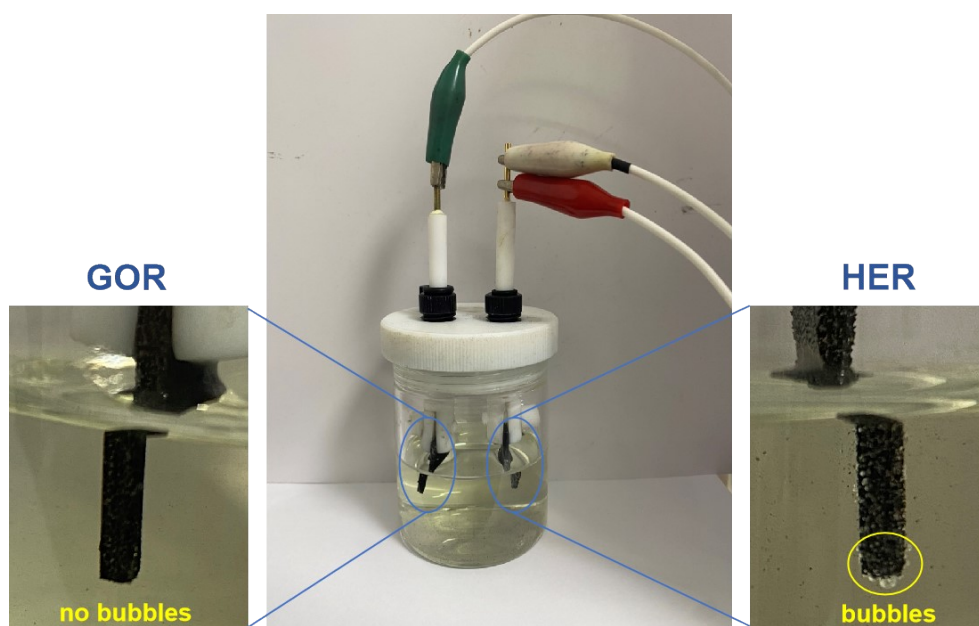**Fig. S9** Optical picture of Bi-Co$_3$O$_4$ NFAs || Bi-Co$_3$O$_4$ NFAs electrolyzer.

Table S1 Performance comparison of Bi-Co$_3$O$_4$ NFAs with Co$_3$O$_4$ NFAs and other recently reported catalysts for GOR and other anodic oxidation reactions.

Reaction type	Catalyst	Potential@10 mA cm^{-2} (V vs. RHE)	Tafel slope (mV dec^{-1})	Electrolyte	Reference
Glucose oxidation reaction (GOR)	Bi-Co$_3$O$_4$ NFAs	1.251	85.9	1 M KOH + 0.15 M glucose	This work
	Co$_3$O$_4$ NFAs	1.257	175.2	1 M KOH + 0.15 M glucose	This work
	Co@NPC	1.460	-	1 M KOH + 0.1 M glucose	[1]
	Ni-MoS$_2$ NPs	1.460	126.4	1 M KOH + 0.3 M glucose	[2]
	Fe$_{0.5}$-CoSe$_2$/CC	1.250	-	1 M KOH + 0.5 M glucose	[3]
	Co@NCNT	1.500	-	1 M KOH + 3 mM glucose	[4]
	Ni/Co Hydro(oxy)oxide porous electrode	1.320	-	1 M KOH + 1 mM glucose	[5]
Urea oxidation reaction (UOR)	NiCo-BDC-S-6	1.326	46.0	1 M KOH + 0.33 M urea	[6]
	Ni(OH)$_2$/NiO-C/WO$_3$ HAs	1.340	99.0	1 M KOH + 0.5 M urea	[7]
	NiSe$_2$-NiMoO$_4$/NF	1.320	33.1	1 M KOH + 0.5 M urea	[8]
	Ni@C-250	1.370	43.0	1 M KOH + 0.5 M urea	[9]
	FeCo-LDH	1.328	85.6	1 M KOH + 0.5 M urea	[10]
Glycerol oxidation reaction (GEOR)	CNs@CoPt	1.320	85.4	1 M KOH + 10 mM glycerol	[11]
	Ni-Mo-N/CFC	1.360	87.0	1 M KOH + 0.1 M glycerol	[12]
	Pd-NCs/NiO-uNPs	1.430	57.5	1 M KOH + 0.5 M glycerol	[13]
	NiO$_x$	1.310	-	1 M KOH + 1 M glycerol	[14]
	HEA-CoNiCuMnMo	1.250	53.4	1 M KOH + 0.1 M glycerol	[15]
5-hydroxymethyl furfura oxidation reaction (HMFOR)	Ni(OH)$_2$-NiOOH/NiFeP	1.350	-	1 M NaOH + 10 mM HFM	[16]
	CoNiP-NIE	1.360	-	1 M NaOH + 10 mM HFM	[17]
	Ni nanosheet/CP	1.410	-	1 M NaOH + 5 mM HFM	[18]
	NiFeCo-LDH	1.530	68.0	1 M NaOH + 5 mM HFM	[19]
	F-doped NiCo$_2$O$_4$	1.388	145.8	1 M KOH + 50 mM HFM	[20]

Table S2 Performance comparison of Bi-Co$_3$O$_4$ NFAs-based GOR-HER electrolyzer with other recently reported electrolyzers.

Catalyst	Cell voltage @10 mA cm^{-2} (V)	Electrolyte	Reference
Bi-Co$_3$O$_4$ NFAs	1.479	1 M KOH + 0.15 M glucose	This work
Co@NPC	1.560	1 M KOH + 0.1 M glucose	[1]
RuCoMn@NC	1.630	1 M KOH + 0.1 M glucose	[21]
Ni-MoS$_2$ NPs	1.670	1 M KOH + 0.3 M glucose	[2]
NiF$_3$/Ni$_2$P@CC	1.540	1 M KOH + 0.33 M urea	[22]
CoS$_2$ NA/Ti	1.590	1 M KOH + 0.3 M urea	[23]
HC-NiMoS/Ti	1.590	1 M KOH + 0.5 M urea	[24]
N-NiS/NiS$_2$	1.620	1 M KOH + 0.33 M urea	[25]
MoO$_2$-FeP@C	1.486	1 M KOH + 10 mM HFM	[26]
Pd-NCs/NiO-uNPs	1.620	1 M KOH + 0.5 M glycerol	[13]

Reference

[1] Li, D., Huang, Y., Li, Z., et al. Deep Eutectic Solvents Derived Carbon-Based Efficient Electrocatalyst for Boosting H_2 Production Coupled with Glucose Oxidation[J]. Chemical Engineering Journal, 2022, 430(1): 132783.

[2] Liu, X., Cai, P., Wang, G., et al. Nickel Doped MoS_2 Nanoparticles as Precious-Metal Free Bifunctional Electrocatalysts for Glucose Assisted Electrolytic H_2 Generation[J]. International Journal of Hydrogen Energy, 2020, 45(58): 32940-32948.

[3] Zheng, D., Li, J., Ci, S., et al. Three-Birds-with-One-Stone Electrolysis for Energy-Efficiency Production of Gluconate and Hydrogen[J]. Applied Catalysis B: Environmental, 2020, 277(1): 119178.

[4] Zhang, E., Xie, Y., Ci, S., et al. Multifunctional High-Activity and Robust Electrocatalyst Derived from Metal-Organic Frameworks[J]. Journal of Materials Chemistry A, 2016, 4(44): 17288-17298.

[5] Chaturvedi, P., Sarker, S., Chen, X., et al. Enhancing the Cooperative Catalytic Effect in Ni/Co Hydr(oxy)oxide Porous Electrodes for Overall Water Splitting and Glucose Sensing[J]. ACS Sustainable Chemistry & Engineering, 2019, 7(13): 11303-11312.

[6] Ao, X., Gu, Y., Li, C., et al. Sulfurization-Functionalized 2D Metal-Organic Frameworks for High-Performance Urea Fuel Cell[J]. Applied Catalysis B: Environmental, 2022, 315(1): 121586.

[7] Zhao, J., Zhang, Y., Guo, H., et al. Defect-Rich $Ni(OH)_2$/NiO Regulated by WO_3 as Core-Shell Nanoarrays Achieving Energy-Saving Water-to-Hydrogen Conversion via Urea Electrolysis[J]. Chemical Engineering Journal, 2022, 433(1): 134497.

[8] Guo, L., Chi, J., Zhu, J., et al. Dual-Doping $NiMoO_4$ with Multi-Channel Structure Enable Urea-Assisted Energy-Saving H_2 Production at Large Current Density in Alkaline Seawater[J]. Applied Catalysis B: Environmental, 2023, 320(1): 121977.

[9] Wang, J., Zhao, Z., Shen, C., et al. Ni/NiO Heterostructures Encapsulated in Oxygen-Doped Graphene as Multifunctional Electrocatalysts for the HER, UOR and HMF Oxidation Reaction[J]. Catalysis Science & Technology, 2021, 11(7): 2480-2490.

[10] Gong, Y., Zhao, H., Ye, D., et al. High Efficiency UOR Electrocatalyst Based on Crossed Nanosheet Structured FeCo-LDH for Hydrogen Production[J]. Applied Catalysis A: General, 2022, 643(1): 118745.

[11] Li, S., Xie, W., Song, Y., et al. Integrated CoPt Electrocatalyst Combined with Upgrading Anodic Reaction to Boost Hydrogen Evolution Reaction[J]. Chemical Engineering Journal, 2022, 437(1): 135473.

[12] Li, Y., Wei, X., Chen, L., et al. Nickel-Molybdenum Nitride Nanoplate Electrocatalysts for Concurrent Electrolytic Hydrogen and Formate Productions[J]. Nature Communications, 2019, 10(1): 5335.

[13] Ma, G., Yang, N., Zhou, G., et al. The Electrochemical Reforming of Glycerol at Pd Nanocrystals Modified Ultrathin NiO Nanoplates Hybrids: An Efficient System for Glyceraldehyde and Hydrogen Coproduction[J]. Nano Research, 2021, 15(3): 1934-1941.

[14] Morales, D. M., Jambrec, D., Kazakova, M. A., et al. Electrocatalytic Conversion of Glycerol to Oxalate on Ni Oxide Nanoparticles-Modified Oxidized Multiwalled Carbon Nanotubes[J]. ACS Catalysis, 2022, 12(2): 982-992.

[15] Fan, L., Ji, Y., Wang, G., et al. High Entropy Alloy Electrocatalytic Electrode toward Alkaline Glycerol Valorization Coupling with Acidic Hydrogen Production[J]. Journal of the American Chemical Society, 2022, 144(16): 7224-7235.

[16] Luo, R., Li, Y., Xing, L., et al. A Dynamic $Ni(OH)_2$-NiOOH/NiFeP Heterojunction Enabling High-Performance E-upgrading of Hydroxymethylfurfural[J]. Applied Catalysis B: Environmental, 2022, 311(1): 121357.

[17] Song, Y., Xie, W., Song, Y., et al. Bifunctional Integrated Electrode for High-Efficient Hydrogen Production Coupled with 5-Hydroxymethylfurfural Oxidation[J]. Applied Catalysis B: Environmental, 2022, 312(1): 121400.

[18] Lu, X., Wu, K. H., Zhang, B., et al. Highly Efficient Electro-reforming of 5-Hydroxymethylfurfural on Vertically Oriented Nickel Nanosheet/Carbon Hybrid Catalysts: Structure-Function Relationships[J]. Angewandte Chemie International Edition, 2021, 60(26):

14528-14535.

[19] Zhang, M., Liu, Y., Liu, B., et al. Trimetallic NiCoFe-Layered Double Hydroxides Nanosheets Efficient for Oxygen Evolution and Highly Selective Oxidation of Biomass-Derived 5-Hydroxymethylfurfural[J]. ACS Catalysis, 2020, 10(9): 5179-5189.

[20] Yang, S., Xiang, X., He, Z., et al. Anionic Defects Engineering of $NiCo_2O_4$ for 5-Hydroxymethylfurfural Electrooxidation[J]. Chemical Engineering Journal, 2023, 457(1): 141344.

[21] Liu, S., Zhang, E., Wan, X., et al. Ru-Co-Mn Trimetallic Alloy Nanocatalyst Driving Bifunctional Redox Electrocatalysis[J]. Science China Materials, 2021, 65(1): 131-138.

[22] Wang, K., Huang, W., Cao, Q., et al. Engineering NiF_3/Ni_2P Heterojunction as Efficient Electrocatalysts for Urea Oxidation and Splitting[J]. Chemical Engineering Journal, 2022, 427(1): 130865.

[23] Wei, S., Wang, X., Wang, J., et al. CoS_2 Nanoneedle Array on Ti Mesh: A Stable and Efficient Bifunctional Electrocatalyst for Urea-Assisted Electrolytic Hydrogen Production[J]. Electrochimica Acta, 2017, 246(1): 776-782.

[24] Wang, X., Wang, J., Sun, X., et al. Hierarchical Coral-Like NiMoS Nanohybrids as Highly Efficient Bifunctional Electrocatalysts for Overall Urea Electrolysis[J]. Nano Research, 2017, 11(2): 988-996.

[25] Liu, H., Liu, Z., Wang, F., et al. Efficient Catalysis of N Doped NiS/NiS_2 Heterogeneous Structure[J]. Chemical Engineering Journal, 2020, 397(1): 125507.

[26] Yang, G., Jiao, Y., Yan, H., et al. Interfacial Engineering of MoO_2-FeP Heterojunction for Highly Efficient Hydrogen Evolution Coupled with Biomass Electrooxidation[J]. Advanced Materials, 2020, 32(17): 2000455.